

Corneal Stress-Strain Index (SSI) Map

Ahmed Abass^{1*}, Ashkan Eliasy¹, Haixia Zhang^{1,2}, Bernardo Lopes¹, Riccardo Vinciguerra^{1,3}, Ahmed Elsheikh^{1,4,5}

¹ School of Engineering, University of Liverpool, Liverpool, L69 3GH, UK, ² School of Biomedical Engineering, Capital Medical University, Beijing Key Laboratory of Fundamental Research on Biomechanics in Clinical Application, Beijing, 100069, China, ³ Department of Ophthalmology, Humanitas San Pio X Hospital, Milan, Italy, ⁴ Beijing Advanced Innovation Centre for Biomedical Engineering, Beihang University, Beijing, 100083, China, ⁵ NIHR Biomedical Research Centre for Ophthalmology, Moorfields Eye Hospital NHS Foundation Trust and UCL Institute of Ophthalmology, UK, *A.Abass@liverpool.ac.uk



Introduction

This study attempts to answer an important question on the regional variation of corneal material stiffness, represented by the Stress-Strain Index (SSI), in both healthy and keratoconic (KC) eyes. It sought to demonstrate how a single SSI value obtained from the CorVis ST (OCULUS Optikgeräte GmbH) for an eye, either healthy or KC, could be translated into a map by adding geometric information and using knowledge about collagen fibril density to show the variation of SSI across corneal surface. This map could enable visualisation of the effect of the disease on the affected area, and help improve fundamental understanding of the mechanics of keratoconus progression in individual patients.

Methods

SSI maps for healthy corneas

Seven healthy corneas were scanned in an earlier study using x-ray scattering to determine their collagen fibril distribution¹. The fibril density at the measurement points, with 0.5 mm spacing in both horizontal and vertical directions, was fitted to Zernike polynomials of the 10th order, and the polynomial coefficients for the seven corneas were averaged to obtain the mean density at each point, Figure 1. The process also allowed determination of the standard deviation (SD) of fibril density at each point, and the mean value of SD (as a percentage of corresponding mean fibril density) across corneal surface was calculated in this study as 2.46±0.39%. This low percentage indicated reasonable consistency of fibril distribution in healthy corneas. The direct link assumed between the fibril density distribution and the material stiffness distribution then enabled estimation of the stiffness variation from one location to another with higher fibril density leading to proportionally higher material stiffness and vice versa.

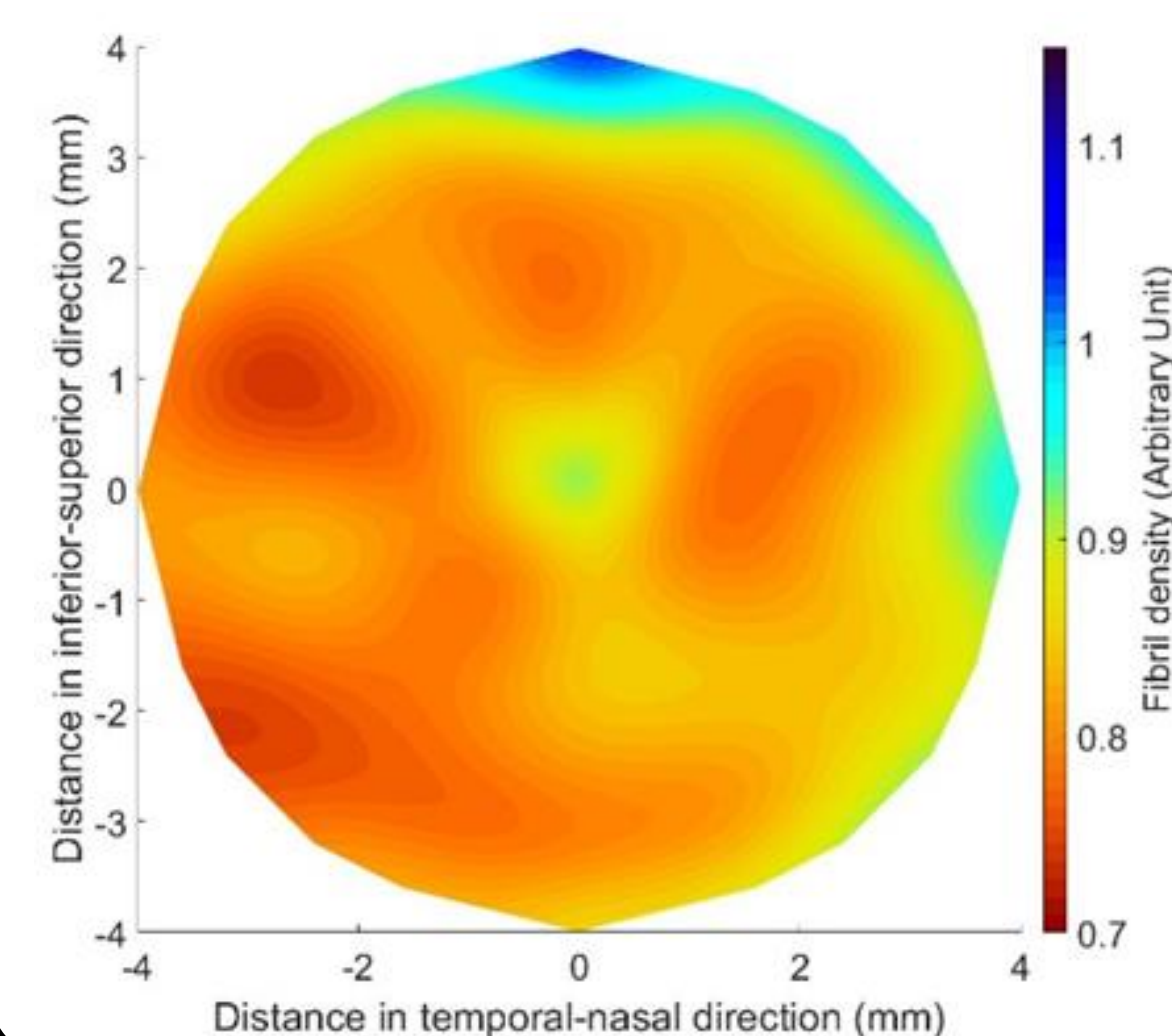


Figure 1 Mean fibril density in the central 8.0 mm diameter area of healthy corneas after being fitted to Zernike polynomials of the 10th order

An inverse analysis process was then established to convert the single SSI reading obtainable with the CorVis ST into an SSI map providing the value of SSI at any point across corneal surface. This process was carried out numerically and was based on an objective function that minimised the difference between the apical displacement under IOP of a cornea model (Model 1) adopting a homogenous material, whose stiffness at all locations originated from the CorVis SSI value, and another cornea model (Model 2), for which the distribution of stiffness followed the mean distribution of fibril density for healthy corneas (Figure 1). The process started with assuming a stiffness level (i.e. a value for SSI, and hence a stress-strain behaviour pattern) at each element integration point in Model 2 while observing that the ratios between these stiffness levels matched the ratios between the fibril contents at the same locations. Depending on how the resulting apical displacement of this model (Model 2) compared with the apical displacement of Model 1 (where all integration points had the same SSI), the stiffness levels adopted in Model 2 were either increased or decreased by the same percentage change. These trials continued until there was a match between the apical displacements of Models 1 and 2, where this match was judged by the following objective function:

$$\text{Root mean square error (RMSE)} = \sqrt{\frac{\sum_{i=1}^n (\delta_{i, \text{Model1}} - \delta_{i, \text{Model2}})^2}{n}}$$

In this equation, δ is the apical displacement of the two models; Model 1 with a homogenous material model, and Model 2 with a stiffness distribution that matched the collagen fibril distribution, i refers to different IOP application steps and n is the total number of IOP steps.

In the analysis, a wide range of the percentage change (used with the stiffness levels in Model 2) was applied and the RMS associated with each change was determined. The percentage change values and the resulting RMS were then fitted to a 3rd order polynomial and the percentage change in stiffness that corresponded to the minimum value of RMS was used to generate the SSI map.

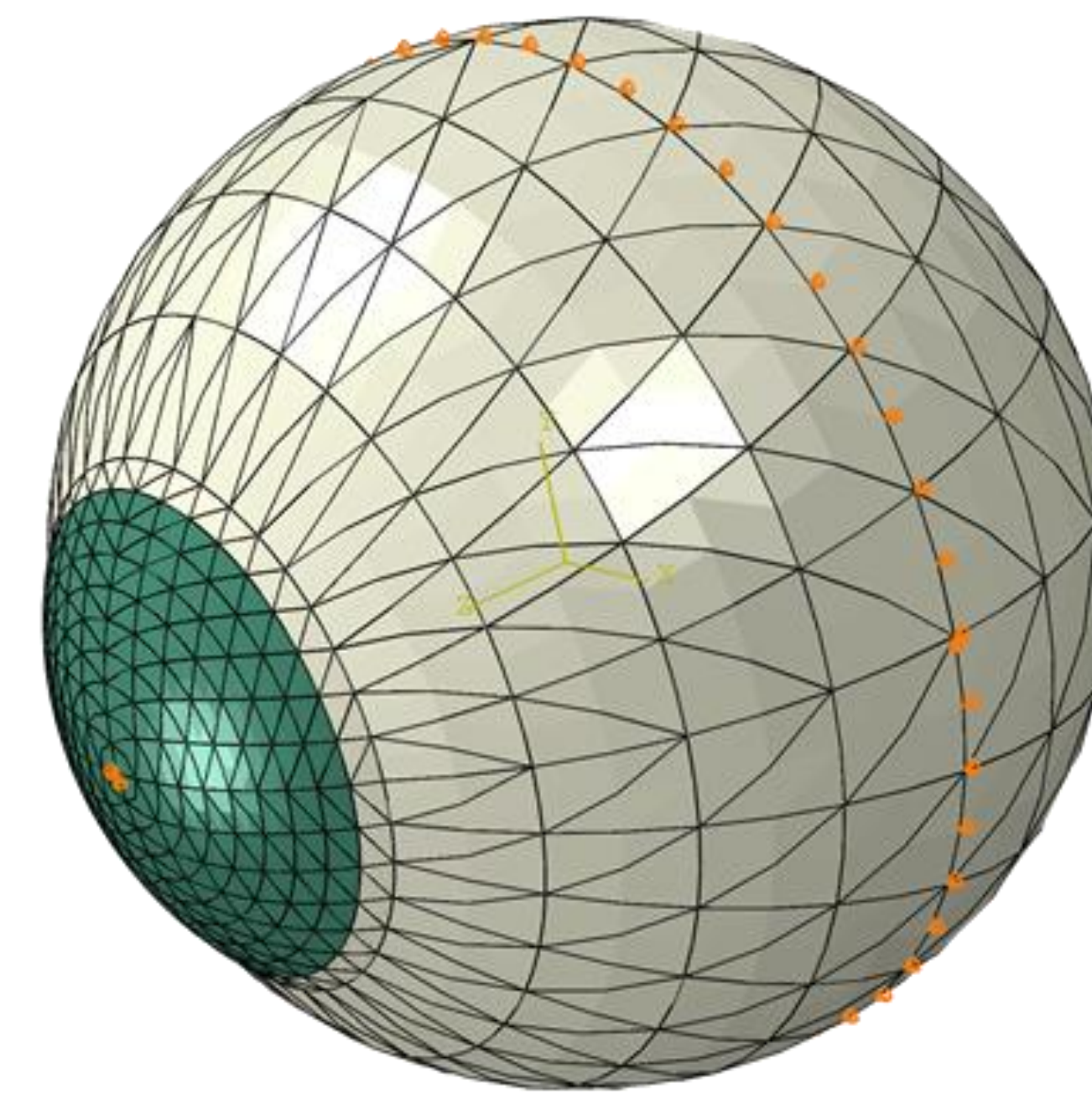


Figure 2 A typical finite element model showing the boundary conditions applied at the equatorial nodes and corneal apex

The numerical models used in the study were finite element (FE) models representing the corneas and matched their assumed geometry (thickness profile, curvature and limbal diameter). The models included 800 fifteen-noded continuum elements organised in one layer, 10 cornea element rings and 10 sclera element rings, Figure 2. The models had a fluid cavity filled with an incompressible fluid with density 1000kg/m³ to simulate the aqueous and the vitreous. IOP was applied through controlling the pressure in this internal fluid. This technique enabled the internal eye pressure to vary from the initial IOP with the deformation experienced under the CorVis air pressure². To prevent rigid body motion, the models were restricted axially (in anterior-posterior direction) at the equatorial nodes, and in both the temporal-nasal and superior-inferior directions at the posterior pole. The FE models adopted a constitutive material model that used the collagen fibril distribution to control the regional and angular variation of stiffness across the tissue surface³. This constitutive model was coded in a custom-built subroutine, which was integrated with the analysis process run on Abaqus FE software (version 6.14, Dassault Systemes Simulia Inc., USA).

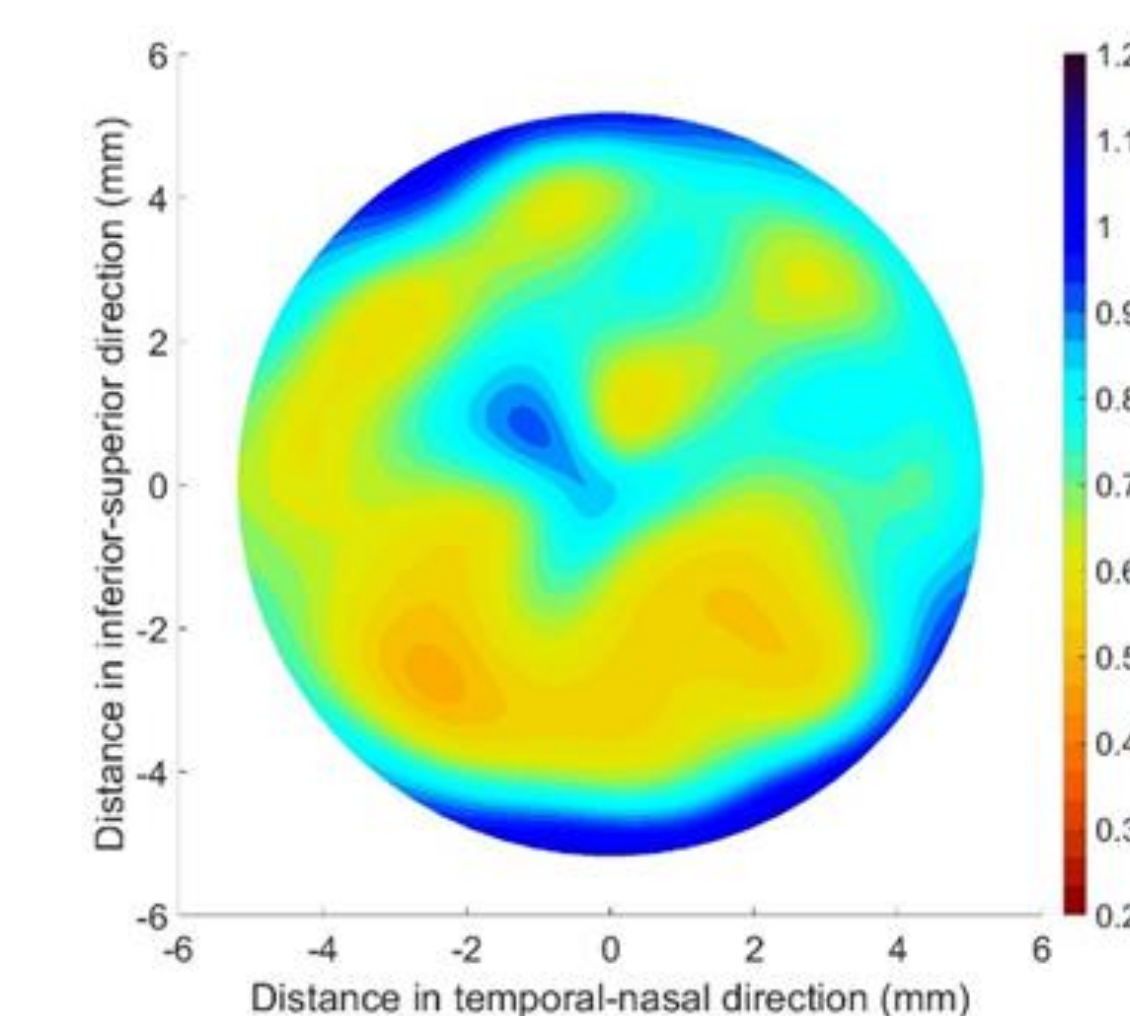
SSI maps for KC corneas

The process to develop SSI maps for KC corneas followed a similar route with two distinctive differences

First, the tomography maps of KC corneas were analysed to determine the height of the cone and the transition region between the cone and outside area using a method developed in an earlier study. This method relied on height information normal to the surface above an optimal sphere to locate the cone centre. It then used the second derivative of height data along equally spaced polar lines originating at the cone centre to locate the cone edge. The second step was to use the outcome of another earlier study to estimate the reduction in fibril density within the cone caused by the disease. This fibril density reduction was based on the cone height and the location of its centre relative to the cornea's apex, in addition to the max curvature of the cornea's anterior surface. Once the fibril reduction in the cone area was estimated, the modelling exercise described above was adopted with no change.

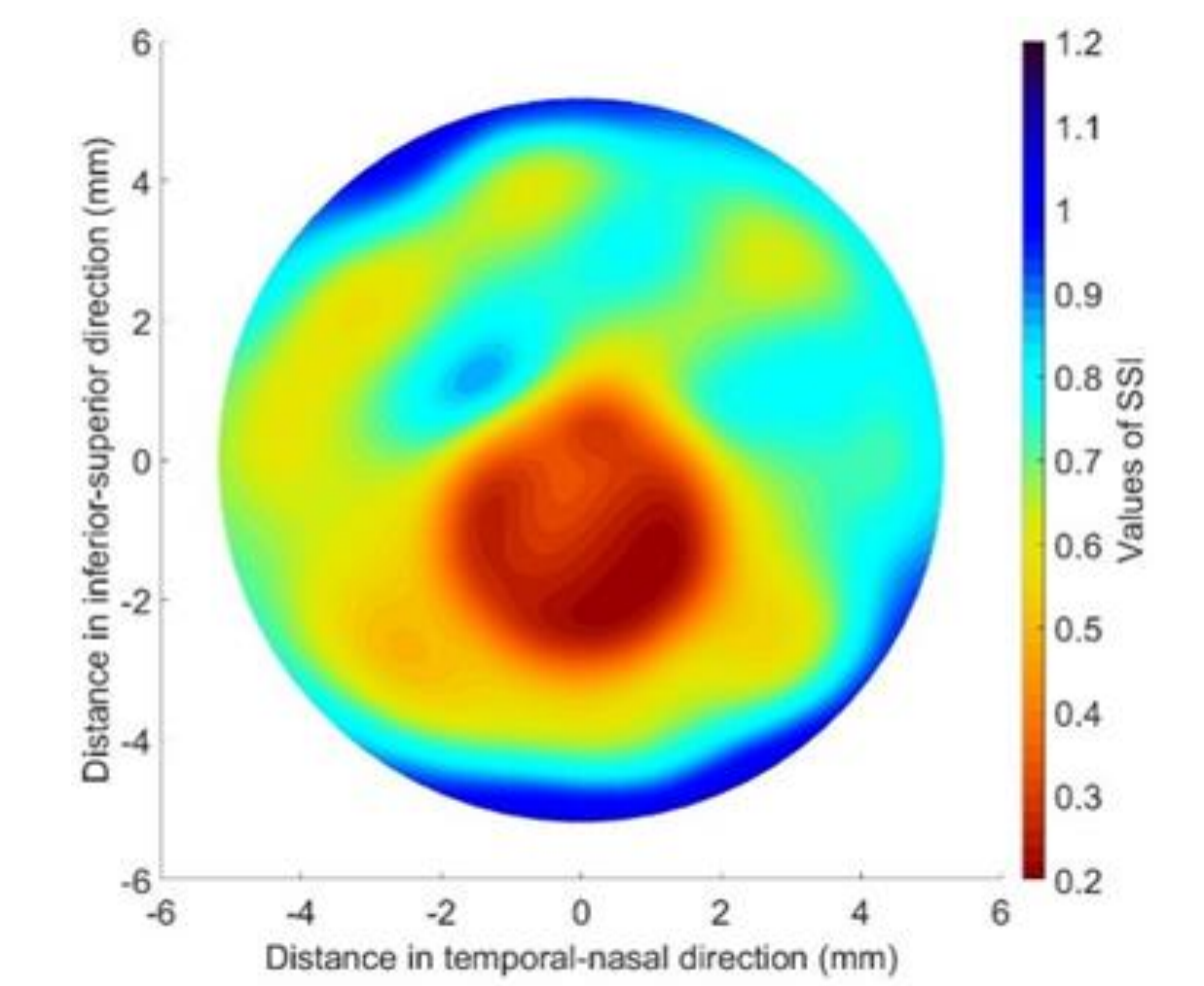
Results

SSI values varied slightly across the corneal surface in healthy eyes. In contrast, keratoconic corneas demonstrated substantial reductions in SSI values inside the cone, Figure 3. These SSI reductions depended on the extent of the disease and increased with more considerable simulated losses in fibril density in the cone area. SSI values and their regional variation showed little change with changes in IOP, corneal thickness and curvature.



(A)

A fibril reduction factor of 0% (Healthy)
Mean ± standard deviation and range of SSI
0.70 ± 0.12 (0.48 - 1.14)



(B)

A fibril reduction factor of 60%
Mean ± standard deviation and range of SSI
0.65 ± 0.19 (0.20 - 1.14)

Figure 3 SSI maps for KC corneas with cones experiencing fibril reductions of 0 (A), and 60% (B). The cones had 2.0 mm radius and were located on the vertical central meridian of the cornea. In all cases, the cones' centers were at 1.0 mm away from the corneal apex.

Conclusion

SSI maps provide an estimation of the regional variation of biomechanical stiffness across the corneal surface. The maps could be particularly useful in keratoconic corneas, demonstrating the dependence of corneal biomechanical behavior on the tissue's microstructure and offering a tool to fundamentally understand the mechanics of keratoconus progression in individual patients.

References

- 1 Zhou, D. et al. Fibril density reduction in keratoconic corneas. J. R. Soc. Interface 18, 175 (2021)
- 2 Eliasy, A. et al. Determination of Corneal Biomechanical Behavior in-vivo for Healthy Eyes Using CorVis ST Tonometry: Stress-Strain Index. Front Bioeng Biotechnol 7, 105 (2019)
- 3 Studer, H. et al. Biomechanical model of human cornea based on stromal microstructure. Journal of biomechanics 43, 836-842 (2010)

Financial Disclosure: This work was funded by Horizon 2020 Framework Programme, European Project "Imcustomeye H2020-ICT-2017", Ref. 779960